Misspecified Cramér-Rao Bound for Terahertz Automotive Radar Range Estimation

Moshe Levy-Israel, Joseph Tabrikian, and Igal Bilik
School of Electrical and Computer Engineering
Ben Gurion University of the Negev, Beer Sheva 84105, Israel
levyismo@post.bgu.ac.il, {joseph, bilik}@bgu.ac.il

***Abstract*—High-resolution information about a host vehicle's surroundings is essential for autonomous driving and advanced driver assistance systems (ADAS). This requires radar systems with high-resolution range, Doppler, azimuth, and elevation capabilities. Terahertz (THz) frequency band radar systems could provide nearly-optical resolution while compact and lightweight. However, frequency-selective range-dependent attenuation of the THz propagation channel challenges the implementation of automotive radars at this frequency band. Estimating the parameters of the THz channel can be computationally complex. Therefore, a flat channel model is conventionally considered for the THz radar range estimator. This work investigates the influence of this assumption on the THz radar range performance estimation via the misspecified Cramér-Rao bound (MCRB). The ability of the proposed approach to evaluate the influence of the frequency-selective misspecification on the radar range estimation accuracy and detection range is evaluated via simulations.**

***Index Terms*—Automotive radar, THz radar, frequency-selective propagation, MCRB, range estimation.**

I. Introduction

Autonomous driving is the main transportation revolution expected to transform our lives in the near future, and advanced driver-assist systems (ADAS) features are already a reality. Autonomous and ADAS vehicles use multiple sensors to monitor the host vehicle's surroundings and detect and avoid hazards [1]. The success of the ADAS and autonomous driving transformation largely depends on the sensing suit performance [2]. Automotive radars play a central role in the autonomous sensing suit [3] since they provide sensing capabilities in any weather and lighting conditions [4, 5]. To enable autonomous driving, they are required to provide high resolution in range, Doppler, azimuth, and elevation [6].

Radar range resolution is determined by the signal bandwidth. State-of-the-art automotive radars operate in the 77 GHz frequency band, where only 4 GHz frequency band is available, which limits their range resolution. Additionally, the Doppler resolution and the angular resolution are proportional to the carrier frequency [7–9].

In order to enhance the radar resolution in range, Doppler, azimuth, and elevation, higher carrier frequencies for radar operation have been proposed [10]. The low-THz frequency band of $100-320$ GHz, midway between the mmW frequency band and optical wavelengths, has been proposed as a potential solution that could satisfy all the sensing requirements for autonomous driving [11–13]. Several studies have demonstrated that THz automotive radars can offer optics-like imaging capabilities while maintaining the advantages of radar systems. THz bands offer wider bandwidths of $10-20$ GHz, allowing for high range accuracy and resolution. The short wavelength of THz radars also permits high angular resolution without increasing the antenna aperture [7–9]. Therefore, THz radar systems can overcome the limitations of current automotive radar systems. THz technology has recently emerged into potential commercial use for terrestrial communications and sensing. Although numerous challenges in the THz radio-frequency (RF) and digital hardware components remain [14], multiple radar system components, such as transceiver [15], modulator [16], antenna [17], antenna arrays [18, 19], and RFCMOS chipsets [20], have already been successfully developed.

Propagation at the THz frequency band is primarily affected by the absorption of water molecules [21]. As a result, the propagation attenuation is nonuniform across the THz band [22]. The propagation attenuation peaks occur at the molecular resonant frequencies. As the number of water molecules between the radar and the target depends on range, range-dependent frequency-selective propagation occurs [23]. In [24], it was shown that the THz range-dependent frequency-selective propagation conditions degrade automotive radar detection and estimation performance due to narrowing the effective bandwidth, spectrum sparsity, and misspecification in the matched-filter receiver.

Lower bounds on the mean-squared error (MSE) estimation are commonly used to predict radar performance and provide a useful tool for system design. The Cramér-Rao bound (CRB) is the most widely used bound on the estimation MSE. It is popular due to its low computational complexity and asymptotic attainability. However, the CRB ignores model misspecification and, therefore, can not be used for analyzing the effects of the THz propagation channel frequency-selectivity on the radar performance. The misspecified CRB (MCRB) has been recently introduced for evaluating the radar performance in scenarios where the model assumed by the estimator differs from the actual model [25–31].

This work proposes an MCRB-based tool to assess the effect of the THz frequency-selectivity in the presence of misspecification. This tool can help decide whether to implement blind methods for channel response estimation and consider the channel response information in the detector. The proposed approach can be used as an operational tool for THz radar design for THz radar performance evaluation and provides

insights into the effects of the THz propagation channel on automotive radar performance.

The rest of the paper is organized as follows. The addressed problem is stated in Section II. Section III presents the radar range estimation approach in the frequency-selective propagation channel in both the misspecified model, which assumes flat-fading propagation, and the perfectly specified model, which assumes knowledge of the frequency-selective propagation profile. The range estimation performance of the THz radar in a typical automotive scenario is evaluated in Section IV, and our conclusions are summarized in Section V.

II. Problem Definition

Consider a single-input single-output (SISO) automotive radar transmitting a base-band signal $s(t)$ towards the target at range r. The base-band radar echo can be modeled as

$$x(t) = \alpha(s * \tilde{h}_\tau)(t) + v(t), \;\; t \in [0, T] \; , \tag{1}$$

where $*$ is the convolution operator, α is an unknown complex attenuation in the propagation channel, $v(\cdot)$ is the additive noise, and T is the observation time. The channel impulse response is $\tilde{h}_\tau(\cdot)$, where $\tau = \frac{2r}{c}$ is the two-way time-delay, and c is the speed of light. Using the Fourier coefficients of the model in (1), it can be obtained that:

$$x_k = \alpha s_k h_k(\tau) e^{-j\omega_k \tau} + v_k, \;\; k = 1, \dots, K \; , \tag{2}$$

where x_k, s_k, v_k, and h_k are the kth Fourier coefficients of the received signal, the transmitted signal, the additive noise, and the channel response $\tilde{h}_\tau(\cdot)$, respectively. The kth angular frequency is denoted by $\omega_k = \frac{2\pi k}{T}$.

Conventional automotive radars at the mmW frequency band typically assume flat-fading propagation conditions, where the channel response is constant over the entire frequency band, $\tilde{h}_\tau(t) = \delta(t - \tau)$, where $\delta(\cdot)$ is the Dirac delta function:

$$x_k = \alpha s_k e^{-j\omega_k \tau} + v_k, \;\; k = 1, \dots, K \; . \tag{3}$$

However, THz automotive radars operate in frequency-selective, range-dependent propagation conditions shown in Fig. 1 that require the matched filter to account for the unknown and frequency-dependent propagation coefficients, $h_k(\tau), \; \forall k = 1, \dots, K$. These coefficients are influenced by several unknown environmental factors and must be estimated. Estimation of the channel parameters may be computationally complex. Implementing the matched-filter based on the radar echo model (3) results in model misspecification. The MCRB bound can then be derived to evaluate the effect of this misspecification on the radar performance. For derivation of the MCRB, the data models from (2) and (3) can be rewritten in vector notation as follows:

$$\tilde{\mathbf{x}} = \alpha \mathbf{E}_\tau \mathbf{H}_\tau \mathbf{s} + \mathbf{v} \; , \tag{4}$$

$$\mathbf{x} = \alpha \mathbf{E}_\tau \mathbf{s} + \mathbf{v} \; , \tag{5}$$

where, $\mathbf{s} = [s_1, \dots, s_K]^T$ is the signal vector, $\mathbf{E}_\tau = \text{diag}\left[e^{-j\omega_1\tau}, \dots, e^{-j\omega_K\tau}\right]$ is the phase shift matrix, and $\mathbf{H}_\tau = \text{diag}\left[h_1(\tau), \dots, h_K(\tau)\right]$ is the channel coefficient matrix. The main objective of this work is to evaluate the radar range estimation performance using the radar echoes that consider the flat-spectrum propagation channel model in (4) when the actual radar echoes experience range-dependent frequency-selective propagation in (5) with unknown parameters:

$$\boldsymbol{\theta} = \left[\boldsymbol{\alpha} \;\; \tau\right]^T \; , \tag{6}$$

where $\boldsymbol{\alpha} \triangleq [\text{Re}\{\alpha\} \;\; \text{Im}\{\alpha\}]$.

III. MCRB Derivation

In the model stated above, the actual probability density function (PDF) of the received radar echoes $g_{\mathbf{x}}(\mathbf{x})$, is unknown. In this case, the maximum likelihood (ML) estimator, $\hat{\boldsymbol{\theta}}$, of the vector, $\boldsymbol{\theta}$, is derived using the assumed PDF, $f_{\mathbf{x}}(\mathbf{x}; \boldsymbol{\theta})$, which may differ from the actual PDF, $f_{\mathbf{x}}(\mathbf{x}; \boldsymbol{\theta}) \neq g_{\mathbf{x}}(\mathbf{x})$. The MCRB provides a lower bound on the MSE of estimators, whose bias adheres to the asymptotic bias of the misspecified ML (MML) estimator [25, 26, 28, 32].

Let the assumed and the actual PDFs of the radar echoes be complex Gaussian, $f_{\mathbf{x}}(\mathbf{x}; \boldsymbol{\theta}) = \mathcal{CN}(\boldsymbol{\mu}(\boldsymbol{\theta}), \mathbf{R})$, and, $g_{\mathbf{x}}(\mathbf{x}) = \mathcal{CN}(\boldsymbol{\mu}', \mathbf{R}')$, where $\boldsymbol{\mu}(\boldsymbol{\theta})$ and $\boldsymbol{\mu}'$ are the mean vectors, and $\mathbf{R}$ and $\mathbf{R}'$ are the covariance matrices. Then, the MCRB for estimating $\boldsymbol{\theta}$ is given by

$$\mathbb{E}_g\left[(\hat{\boldsymbol{\theta}} - \boldsymbol{\theta})(\hat{\boldsymbol{\theta}} - \boldsymbol{\theta})^T\right] \succcurlyeq \underbrace{\mathbf{A}^{-1}(\boldsymbol{\theta})\mathbf{B}(\boldsymbol{\theta})\mathbf{A}^{-1}(\boldsymbol{\theta})}_{(a)} + \underbrace{(\boldsymbol{\theta} - \boldsymbol{\theta}_A)(\boldsymbol{\theta} - \boldsymbol{\theta}_A)^T}_{(b)} \; , \tag{7}$$

where (a) expresses the covariance contribution and (b) the model misspecification bias. The term $\mathbf{B}(\boldsymbol{\theta})$ in (7) can be obtained by the generalized Slepian-Bangs formula [25]:

$$\mathbf{B}(\boldsymbol{\theta}) = 2\text{Re}\left\{\nabla\boldsymbol{\mu}^H(\boldsymbol{\theta})\mathbf{R}^{-1}\mathbf{R}'\mathbf{R}^{-1}\nabla\boldsymbol{\mu}(\boldsymbol{\theta})\right\} \; , \tag{8}$$

and the elements of $\mathbf{A}(\boldsymbol{\theta})$ are given by

$$A_{ij} = B_{ij} - 2\text{Re}\left\{\frac{\partial^2\boldsymbol{\mu}^H(\boldsymbol{\theta})}{\partial\xi_i\partial\xi_j}\mathbf{R}^{-1}\Delta\boldsymbol{\mu}\right\} \; , \tag{9}$$

where

$$\Delta\boldsymbol{\mu} \triangleq \boldsymbol{\mu}' - \boldsymbol{\mu}(\boldsymbol{\theta}) \; , \tag{10}$$

and $\boldsymbol{\theta}_A$ is the ML convergence point, which introduces bias due to model misspecification:

$$\boldsymbol{\theta}_A \triangleq \arg\min_{\boldsymbol{\theta}'} \text{KLD}(g_{\mathbf{x}}(\mathbf{x}) \| f_{\mathbf{x}}(\mathbf{x}, \boldsymbol{\theta}')), \tag{11}$$

and $\text{KLD}(\cdot\|\cdot)$ denotes the Kullback-Leibler divergence. In the considered problem, the difference between the assumed model in (5), and the actual model in (4), is the expectation component of the radar echoes PDFs in (10), while the covariance components are identical. Therefore, (8) can be rewritten as:

$$\mathbf{B}(\boldsymbol{\theta}) = 2\text{Re}\left\{\nabla\boldsymbol{\mu}^H(\boldsymbol{\theta})\mathbf{R}^{-1}\nabla\boldsymbol{\mu}(\boldsymbol{\theta})\right\} \triangleq \mathbf{J}(\boldsymbol{\theta}) \; , \tag{12}$$

which is identical to the Fisher information matrix (FIM) of the data model in (5). Notice that without loss of generality, the radar echoes can be spatially whitened as:

$$\mathbf{R} = \sigma_{\mathbf{v}}^2\mathbf{I}_K \; . \tag{13}$$

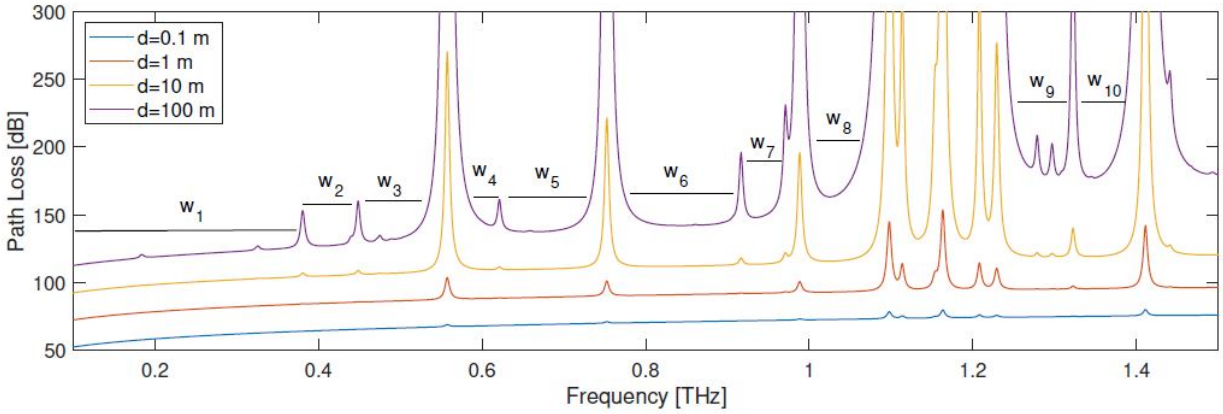

Fig. 1. Path loss of the frequency-selective range-dependent THz propagation channel [23].

Using (13) and by substitution of the expectation of the data model from (5) in (12), one obtains

$$\mathbf{J}(\boldsymbol{\theta}) = \frac{2}{\sigma_v^2}\mathrm{Re}\left\{\frac{\partial\left(\alpha\mathbf{E}_\tau\mathbf{s}\right)^H}{\partial\boldsymbol{\theta}}\frac{\partial\alpha\mathbf{E}_\tau\mathbf{s}}{\partial\boldsymbol{\theta}}\right\}$$
$$= \frac{2}{\sigma_v^2}\mathrm{Re}\left\{\left[\mathbf{E}_\tau\mathbf{s}\; j\mathbf{E}_\tau\mathbf{s}\; -j\alpha\boldsymbol{\Omega}\mathbf{E}_\tau\mathbf{s}\right]^H\left[\mathbf{E}_\tau\mathbf{s}\; j\mathbf{E}_\tau\mathbf{s}\; -j\alpha\boldsymbol{\Omega}\mathbf{E}_\tau\mathbf{s}\right]\right\}$$
$$= \frac{2}{\sigma_v^2}\mathrm{Re}\left\{\begin{pmatrix}\|\mathbf{s}\|^2 & 0 & -j\alpha\rho_{s\omega s}\\ 0 & \|\mathbf{s}\|^2 & -\alpha\rho_{s\omega s}\\ j\alpha^*\rho_{s\omega s} & -\alpha^*\rho_{s\omega s} & |\alpha|^2\rho_{s\omega^2 s}\end{pmatrix}\right\}, \quad (14)$$

where $\boldsymbol{\Omega} = \mathrm{diag}\left(\omega_1,\ldots,\omega_K\right)$, $\rho_{s\omega s} = \mathbf{s^H\Omega s}$, and $\rho_{s\omega^2 s} = \mathbf{s^H\Omega^2 s}$. The CRB for estimating τ is

$$\mathrm{CRB}_{\mathbf{xx}} = \frac{1}{2\mathrm{SNR}}\frac{1}{\left(\rho_{s\omega^2 s} - \frac{|\rho_{s\omega s}|^2}{\|\mathbf{s}\|^2}\right)}, \quad (15)$$

where the signal-to-noise ratio (SNR) is defined as $\mathrm{SNR} = \frac{|\alpha|^2}{\sigma_v^2}$.

Similarly, defining $\tilde{\mathbf{s}} = \mathbf{H}_\tau\mathbf{s}$ in (15), the CRB for the frequency-selective model in (4) is given by

$$\mathrm{CRB}_{\tilde{\mathbf{x}}\tilde{\mathbf{x}}} = \frac{1}{2\mathrm{SNR}}\frac{1}{\left(\rho_{\tilde{\mathbf{s}}\omega^2\tilde{\mathbf{s}}} - \frac{|\tilde{\mathbf{s}}^H\boldsymbol{\Omega}\tilde{\mathbf{s}}|^2}{\|\tilde{\mathbf{s}}\|^2}\right)}, \quad (16)$$

where $\rho_{\tilde{s}\omega\tilde{s}} = \mathbf{s}^H\mathbf{H}_\tau^H\boldsymbol{\Omega}\mathbf{H}_\tau\mathbf{s}$. Notice that $\mathrm{CRB}_{\tilde{\mathbf{x}}\tilde{\mathbf{x}}}$ is the lower bound on the range estimation error, assuming perfect knowledge of the channel response, $\tilde{h}(\tau)$. However, obtaining accurate knowledge of the channel response involves additional estimation that may be computationally complex. Moreover, there could be scenarios when the contribution of this knowledge to the target range estimation is insignificant and does not justify the additional computational burden. The MCRB can assess the radar range performance degradation due to the mismatch between the actual and the considered models. Therefore, it can be used to decide on the need for the actual model parameters estimation at the expense of additional computational complexity.

Using the relations,

$$\boldsymbol{\mu}(\boldsymbol{\theta}) = \alpha\mathbf{E}_\tau\mathbf{s}\,, \quad (17)$$
$$\boldsymbol{\mu}' = \alpha\mathbf{E}_\tau\mathbf{H}\mathbf{s}\,, \quad (18)$$
$$\Delta\boldsymbol{\mu} = \alpha\mathbf{E}_\tau\left(\mathbf{H}_\tau - \mathbf{I}\right)\mathbf{s}\,, \quad (19)$$

the KLD in (11) can be minimized by τ' that maximizes the inner product between $\boldsymbol{\mu}$ and $\boldsymbol{\mu}'$ as follows:

$$\tau_A = \arg\max_{\tau'}\left|\mathbf{s}^H\mathbf{E}_{\tau'}^*\mathbf{E}_\tau\mathbf{H}_\tau\mathbf{s}\right|^2. \quad (20)$$

Using (17)-(20) in (7) and in (9), obtain

$$\mathrm{MCRB} = \left[\mathbf{A}^{-1}(\boldsymbol{\theta})\mathbf{J}(\boldsymbol{\theta})\mathbf{A}^{-1}(\boldsymbol{\theta})\right]_{33} + \left(\tau - \tau_A\right)^2, \quad (21)$$

where $[\cdot]_{k,k}$ is the (k,k)th matrix element and

$$\mathbf{A}(\boldsymbol{\theta}) = \frac{2}{\sigma_v^2}\mathrm{Re}\left\{\begin{pmatrix}\|\mathbf{s}\|^2 & 0 & -j\alpha\rho_{s\omega\tilde{s}}\\ 0 & \|\mathbf{s}\|^2 & \alpha\rho_{s\omega\tilde{s}}\\ -j\alpha\rho_{s\omega\tilde{s}} & \alpha\rho_{s\omega\tilde{s}} & |\alpha|^2\rho_{s\omega^2\tilde{s}}\end{pmatrix}\right\}, \quad (22)$$

where $\rho_{s\omega\tilde{s}} = \mathbf{s}^H\boldsymbol{\Omega}\mathbf{H}_\tau\mathbf{s}$ and $\rho_{s\omega^2\tilde{s}} = \mathbf{s}^H\boldsymbol{\Omega}^2\mathbf{H}_\tau\mathbf{s}$.

This work examines the range estimation performance of three matched-filter (MF) range estimators. The conventional MF, derived for flat-fading propagation channel, corresponding to the CRB in (15), is given by

$$\hat{r}_{ML} = \arg\max_{\tau'}\left|\mathbf{s}^H\mathbf{E}_{\tau'}^*\mathbf{x}\right|^2. \quad (23)$$

The second range estimator considers the frequency-selective propagation channel where the channel is perfectly known to the estimator, corresponding to the CRB in (16), is given by

$$\hat{r}_{PML} = \arg\max_{\tau'}\left|\mathbf{s}^H\mathbf{H}_\tau^H\mathbf{E}_{\tau'}^*\tilde{\mathbf{x}}\right|^2. \quad (24)$$

Finally, the third range estimator for the frequency-selective propagation channel considers the flat-fading channel model corresponding to the MCRB in (21), is

$$\hat{r}_{MML} = \arg\max_{\tau'}\left|\mathbf{s}^H\mathbf{E}_{\tau'}^*\tilde{\mathbf{x}}\right|^2. \quad (25)$$

IV. THz Automotive Radar Performance Evaluation

In this section, we investigate the ability of the proposed MCRB to evaluate the radar range estimation performance in frequency-selective THz propagation channels. The frequency-selective THz channel propagation loss phenomenon is illustrated in Fig. 1. We simulate the channel using Beer-Lambert law [23] with attenuation range profile determined by $\beta_k = 0.1\cos\left(\frac{\pi k}{2K}\right)$, where the number of frequency bins is set to $K = 256$. It is evident from (20) that when dealing with a real channel, i.e., $\mathrm{Im}\{\mathbf{H}_\tau\} = \mathbf{0}$, which is the case in our simulation, the bias term becomes zero, indicating that τ_A is equal to τ.

Fig. 2 shows the root-MSE (RMSE) of the three range estimators presented in (23), (24), and (25) and compare them to their corresponding CRBs and MCRB in (15), (16), and (21), respectively. This figure shows that given sufficiently high SNR, all the considered estimators achieve their corresponding bounds. Notice that the threshold of the MML estimator is only 5 dB higher than that of the PML, while the MCRB is shifted by 9 dB in SNR. Although the MCRB, similarly to the CRB, can not predict the threshold, this experiment proves the feasibility of using the MCRB as a useful tool for evaluating the range estimation performance degradation due to the frequency-selective THz propagation conditions. Comparison between the $\mathrm{CRB}_{\tilde{\mathbf{x}}\tilde{\mathbf{x}}}$ with the MCRB shows that by using the MF that relies on the perfect knowledge of the channel, one may prove the performance by about 9 dB in SNR. However, it requires estimation of the channel response, which is range-dependent, and implementation of a more complex MF, increasing the computational complexity, which can be impractical. The information provided by the MCRB on the SNR loss due to the model mismatch can be used to assess the trade-off between the performance improvement and the associated computational complexity.

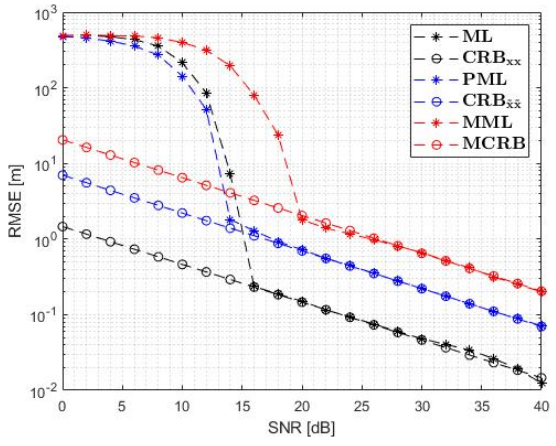

Fig. 2. Range estimation RMSE versus SNR, for a target located at $r = 50$ meters, with the corresponding channel response

V. Conclusion

This work addressed the frequency-selective propagation conditions that challenge the THz automotive radar operation. Implementing an accurate fast-time matched-filter, which considers the channel frequency response, is computationally complex. The MCRB-based approach to evaluate the influence of the frequency-selective THz propagation model mismatch on the radar range estimation performance is introduced. It was shown via simulations that the proposed approach can efficiently evaluate the influence of the propagation channel mismatch and therefore be used to decide on the need for the complex channel-matched filter receiver implementation.

References

[1] H. Meinel and J. Dickman, "Automotive radar: from its origin to future directions," *Microwave Journal*, vol. 56, no. 9, pp. 24–40, 2013.

[2] A. Modas, R. Sanchez-Matilla, P. Frossard, and A. Cavallaro, "Toward robust sensing for autonomous vehicles: An adversarial perspective," *IEEE Signal Processing Magazine*, vol. 37, no. 4, pp. 14–23, 2020.

[3] H. H. Meinel, "Evolving automotive radar — from the very beginnings into the future," in *The 8th European Conference on Antennas and Propagation (EuCAP 2014)*, 2014, pp. 3107–3114.

[4] M. Murad, I. Bilik, M. Friesen, J. Nickolaou, J. Salinger, K. Geary, and J. Colburn, "Requirements for next generation automotive radars," in *Radar Conference (RADAR), 2013 IEEE*. IEEE, 2013, pp. 1–6.

[5] I. Bilik, O. Bialer, S. Villeval, H. Sharifi, K. Kona, M. Pan, D. Persechini, M. Musni, and K. Geary, "Automotive MIMO radar for urban environments," in *Radar Conference (RadarConf), 2016 IEEE*. IEEE, 2016, pp. 1–6.

[6] I. Bilik, O. Longman, S. Villeval, and J. Tabrikian, "The rise of radar for autonomous vehicles: Signal processing solutions and future research directions," *IEEE Signal Processing Magazine*, vol. 36, no. 5, pp. 20–31, 2019.

[7] E. Marchetti, R. Du, B. Willetts, F. Norouzian, E. G. Hoare, T. Y. Tran, N. Clarke, M. Cherniakov, and M. Gashinova, "Radar cross-section of pedestrians in the low-THz band," *IET Radar, Sonar & Navigation*, vol. 12, no. 10, pp. 1104–1113, 2018.

[8] M. Sheeny, A. Wallace, and S. Wang, "300 GHz radar object recognition based on deep neural networks and transfer learning," *IET Radar, Sonar & Navigation*, vol. 14, no. 10, pp. 1483–1493, 2020.

[9] E. Marchetti, S. Cassidy, F. Norouzian, E. Hoare, M. Cherniakov, and M. Gashinova, "Automotive targets characterization in the low-THz band," in *IEEE International Radar Symposium*, 2019, pp. 1–6.

[10] S. H. Dokhanchi, B. S. Mysore, K. V. Mishra, and B. Ottersten, "A mmWave automotive joint radar-communications system," *IEEE Transactions on Aerospace and Electronic Systems*, vol. 55, no. 3, pp. 1241–1260, 2019.

[11] F. Norouzian, E. Hoare, E. Marchetti, M. Cherniakov, and M. Gashinova, "Next generation, low-THz automotive radar–The potential for frequencies above 100 GHz," in *IEEE International Radar Symposium*, 2019, pp. 1–7.

[12] A. M. Elbir, K. V. Mishra, and S. Chatzinotas, "Terahertz-band joint ultra-massive MIMO radar-communications: Model-based and model-free hybrid beamforming," *arXiv preprint arXiv:2103.00328*, 2021.

[13] Y. Xiao, F. Norouzian, E. G. Hoare, E. Marchetti, M. Gashinova, and M. Cherniakov, "Modeling and experiment verification of transmissivity of low-THz radar signal through vehicle infrastructure," *IEEE Sensors Journal*, vol. 20, no. 15, pp. 8483–8496, 2020.

[14] D. Saeedkia, *Handbook of terahertz technology for imaging, sensing and communications*. Elsevier, 2013.

[15] J. M. Jornet and I. F. Akyildiz, "Graphene-based plasmonic nano-antenna for terahertz band communication in nanonetworks," *IEEE Journal on Selected Areas in Communications*, vol. 31, no. 12, pp. 685–694, 2013.

[16] L. Valzania, Y. Zhao, L. Rong, D. Wang, M. Georges, E. Hack, and P. Zolliker, "THz coherent lensless imaging," *Applied optics*, vol. 58, no. 34, pp. G256–G275, 2019.

[17] K. Konstantinidis, A. P. Feresidis, C. C. Constantinou, E. Hoare, M. Gashinova, M. J. Lancaster, and P. Gardner, "Low-THz dielectric lens antenna with integrated waveguide feed," *IEEE Transactions on Terahertz Science and Technology*, vol. 7, no. 5, pp. 572–581, 2017.

[18] L.-H. Gao, Q. Cheng, J. Yang, S.-J. Ma, J. Zhao, S. Liu, H.-B. Chen, Q. He, W.-X. Jiang, H.-F. Ma *et al.*, "Broadband diffusion of terahertz waves by multi-bit coding metasurfaces," *Light: Science & Applications*, vol. 4, no. 9, pp. e324–e324, 2015.

[19] A. Singh, M. Andrello, E. Einarsson, N. Thawdarl, and J. M. Jornet, "A hybrid intelligent reflecting surface with graphene-based control elements for THz communications," in *IEEE International Workshop on Signal Processing Advances in Wireless Communications*, 2020, pp. 1–5.

[20] S. Kueppers, R. Herschel, S. Wang, D. Nüer, and N. Pohl, "Imaging characteristics of a 24× 24 channel MIMO FMCW radar based on a SiGe: C chipset," in *IEEE MTT-S International Microwave Workshop Series on Advanced Materials and Processes for RF and THz Applications*, 2019, pp. 133–135.

[21] J. M. Jornet and I. F. Akyildiz, "Channel modeling and capacity analysis for electromagnetic wireless nanonetworks in the terahertz band," *IEEE Transactions on Wireless Communications*, vol. 10, no. 10, pp. 3211–3221, 2011.

[22] R. Goody and Y. Yung, *Atmospheric Radiation: Theoretical Basis*. OUP USA, 1995. [Online]. Available: https://books.google.co.il/books?id=e3U8DwAAQBAJ

[23] Z. Hossain and J. M. Jornet, "Hierarchical bandwidth modulation for ultra-broadband Terahertz communications," in *IEEE International Conference on Communications*, 2019, pp. 1–7.

[24] J. Tabrikian and I. Bilik, "Range estimation in frequency-selective propagation environment for terahertz automotive radar," in *2022 IEEE 12th Sensor Array and Multichannel Signal Processing Workshop (SAM)*, 2022, pp. 76–80.

[25] C. D. Richmond and L. L. Horowitz, "Parameter bounds on estimation accuracy under model misspecification," *IEEE Transactions on Signal Processing*, vol. 63, no. 9, pp. 2263–2278, 2015.

[26] Q. H. Vuong, "Cramér-Rao bounds for misspecified models (working paper 652)," *Division of the Humanities and Social Sciences, California Institute of Technology*, 1986.

[27] S. Fortunati, F. Gini, M. S. Greco, and C. D. Richmond, "Performance bounds for parameter estimation under misspecified models: Fundamental findings and applications," *IEEE Signal Processing Magazine*, vol. 34, no. 6, pp. 142–157, 2017.

[28] Q. Ding and S. Kay, "Maximum likelihood estimator under a misspecified model with high signal-to-noise ratio," *IEEE Transactions on Signal Processing*, vol. 59, no. 8, pp. 4012–4016, 2011.

[29] S. Fortunati, F. Gini, and M. Greco, "The misspecified Cramér-Rao bound and its application to scatter matrix estimation in complex elliptically symmetric distributions," *IEEE Trans. Signal Process.*, vol. 64, no. 9, p. 2387–2399, 2016.

[30] A. Mennad, S. Fortunati, M. N. E. Korso, A. Younsi, A. M. Zoubir, and A. Renaux, "Slepian-Bangs-type formulas and the related misspecified Cramér-Rao bounds for complex elliptically symmetric distributions," *Signal Processing*, vol. 142, pp. 320 – 329, 2018.

[31] M. Levy-Israel, I. Bilik, and J. Tabrikian, "Misspecified cramér-rao bound for multipath model in mimo radar," in *2022 IEEE 12th Sensor Array and Multichannel Signal Processing Workshop (SAM)*, 2022, pp. 81–85.

[32] S. Fortunati, "Misspecified Cramér–Rao bounds for complex unconstrained and constrained parameters," *in Proc. Eur. Signal Process. Conf.*, 2017.